

Modeling of Transport through Submicron Semiconductor Structures: A Direct Solution of the Coupled Poisson-Boltzmann Equations

D. CSONTOS AND S.E. ULLOA

*Department of Physics and Astronomy, and Nanoscale and Quantum Phenomena Institute, Ohio University,
Athens, Ohio 45701, USA*
csontos@phy.ohiou.edu

Abstract. We report on a computational approach based on the self-consistent solution of the steady-state Boltzmann transport equation coupled with the Poisson equation for the study of inhomogeneous transport in deep submicron semiconductor structures. The nonlinear, coupled Poisson-Boltzmann system is solved numerically using finite difference and relaxation methods. We demonstrate our method by calculating the high-temperature transport characteristics of an inhomogeneously doped submicron GaAs structure where the large and inhomogeneous built-in fields produce an interesting fine structure in the high-energy tail of the electron velocity distribution, which in general is very far from a drifted-Maxwellian picture.

Keywords: Boltzmann equation, electron distribution function, submicron devices, upwind method

1. Introduction

The carrier dynamics in submicron structures is far from thermal equilibrium due to strong and rapidly varying external and built-in electric fields. Hot electron and ballistic effects dominate the transport characteristics and the electron velocity distribution function in such systems is far from a drifted-Maxwellian description. In order to fully take into account the nonequilibrium nature of the transport, a full solution of the semiclassical Boltzmann transport equation (BTE) is required. Although the Monte Carlo method has been very popular for the solution of the BTE in semiconductor device simulation [1], several works [2]-[7] have recently solved the BTE by direct methods, thus allowing noise-free spatial and temporal resolution of the electron distribution function, which in the Monte Carlo method may be difficult to obtain due to the statistical nature of the approach. In this paper, we present a straight-forward approach to calculate the electron distribution function, $f(x, v)$, for submicron inhomogeneous semiconductor structures by solving the steady-state BTE self-consistently with the Poisson equation. We solve the strictly two-dimensional

(2D) BTE (one dimension corresponding to position and one to velocity) and treat scattering within the relaxation time approximation (RTA) where each individual scattering mechanism is represented by a characteristic scattering rate that can be derived from quantum mechanical scattering theory. We demonstrate our approach for submicron, inhomogeneously doped structures and discuss the general nonequilibrium transport characteristics.

2. Basic equations

The Boltzmann equation describes the dynamics of the semiclassical distribution function, $f(\mathbf{r}, \mathbf{v}, t)$, under the influence of electric and magnetic fields, as well as different scattering processes. In the absence of a magnetic field, the 2D phase-space, steady-state BTE in the RTA is written according to:

$$-\frac{eE(x)}{m^*} \frac{\partial f(x, v)}{\partial v} + v \frac{\partial f(x, v)}{\partial x} = -\frac{f(x, v) - f_{LE}(x, v)}{\tau(\varepsilon)}, \quad (1)$$

where m^* is the electron effective mass in the parabolic band approximation, and $f_{LE}(x, v)$ is a local equilibrium distribution function appropriate to a local den-

sity, applied field and equilibrium lattice temperature, T_0 , to which the distribution function $f(x, v)$ relaxes at a relaxation rate $\tau(\varepsilon)^{-1}$. As the local equilibrium function, we choose in the following a Maxwell-Boltzmann (MB) distribution at T_0 , normalized to the local density $n(x)$

$$f_{LE}(x, v) = n(x) \left[\frac{m^*}{2\pi k T_0} \right]^{1/2} e^{-\frac{m^* v^2}{2k_B T_0}}. \quad (2)$$

The inhomogeneous electric field, $E(x)$, in the BTE, originating from the spatially dependent electron and doping densities, $n(x)$ and $N_D(x)$, is obtained from the Poisson equation

$$\frac{d^2\phi}{dx^2} = -\frac{dE}{dx} = -e \frac{N_D(x) - n(x)}{\epsilon \epsilon_0} = -\rho(x), \quad (3)$$

where ϵ is the static dielectric constant. Since the electron density is related to the distribution function by

$$n(x) = \int_{-\infty}^{\infty} f(x, v) dv, \quad (4)$$

the Poisson and Boltzmann equations constitute a coupled, nonlinear set of equations, and thus, Eqs. (1-4) have to be solved self-consistently.

3. Numerical procedure

The numerical procedure consists, in short, of initializing the system parameters, discretizing Eqs. (1-4) on a 2D grid in phase-space, performing the self-consistent Poisson-Boltzmann loop and, upon convergence, calculate and output the electron distribution function, electric field and the desired moments of the BTE. In the calculations, after initialization, we rescale the system parameters and the equations according to

$$x' = x/L_D, \quad v' = v\tau/L_D, \quad (5)$$

where $L_D = \sqrt{\epsilon \epsilon_0 k_B T_0 / e^2 N}$ is the Debye length, $N = \max[N_D(x)]$ and τ is a characteristic scattering time. The choice of grid size and resolution depends to a large extent on the system parameters and the electrostatics present in the device. In order to reproduce details due to strong and rapidly varying electric fields, we choose the spatial grid step size to be smaller than the Debye length, L_D , defined above. In velocity space, on the other hand, the discrete grid step size needs to be small enough to resolve fine structure in the distribution function, as well as give accurate results for the moments of the BTE. In addition, the

grid needs to be large enough, in velocity, in order to capture the full information in the high-energy tail of the distribution function, and in position, in order to damp out the effects of the contact boundaries.

The Poisson and Boltzmann equations are solved by finite difference and iterative relaxation methods [8]. For the Poisson equation (3), we use forward and backward Euler differences according to

$$L_x^+ L_x^- \phi_j = \frac{\phi_{j+1} - 2\phi_j + \phi_{j-1}}{(\delta x)^2} = -\rho_j, \quad (6)$$

where $L_x^+ \phi(x) = (\phi_{j+1} - \phi_j)/\delta x$ and $L_x^- \phi(x) = (\phi_j - \phi_{j-1})/\delta x$ denote forward and backward Euler steps, respectively. The resulting matrix equation is solved iteratively using successive overrelaxation (SOR) [8].

For the solution of the BTE, we adopt an upwind finite difference scheme [3] which amounts to the following discretization of the partial derivatives in Eq. (1):

$$\frac{\partial f}{\partial v} = L_v^{+[-]} f(x, v) \quad E(x) > 0 \quad [E(x) \leq 0] \quad (7)$$

$$\frac{\partial f}{\partial x} = L_x^{+[-]} f(x, v) \quad v < 0 \quad [v \geq 0]. \quad (8)$$

As for the Poisson equation, we use SOR to solve the matrix equation resulting from the discretization of Eq. (1).

For the boundary conditions of the Poisson-Boltzmann equations we adopt the following: For the potential, the values at the system boundaries, denoted (l)eft and (r)ight are fixed to $\phi(x_l) = U_0$ and $\phi(x_r) = 0$, respectively, corresponding to an externally applied voltage U_0 . The electron density is allowed to fluctuate freely around the boundaries, subject to the condition of global charge neutrality, which is enforced between each successive iteration in the self-consistent Poisson-Boltzmann loop. We choose the size of the highly-doped contacts to be large enough such that the electron density and the electric field deep inside the contacts is constant.

For the electron distribution function four boundary conditions can be defined in the 2D phase-space. At the velocity cut-off in phase-space, we choose $f(x, v_{max}) = f(x, -v_{max}) = f_{LE}(x, v)$ which is reasonable since we assume $v_{max} \geq 30k_B T_0$ in the calculations. At such high velocities, the electron population is negligible and of the same order as the local equilibrium distribution $f_{LE}(x, v)$. At the contact boundaries, we assume that the electric field is low and constant (as verified in the calculations), and thus,

the homogeneous solution to the BTE in the linear response regime of transport applies. Hence,

$$f(x_i, v) = f_{LE}(x_i, v)[1 - vE(x_i)\tau(\varepsilon)/k_B T_0], \quad (9)$$

where $i = l, r$. The iterative Poisson-Boltzmann loop consists of an updating procedure for the electric field, electron distribution function and electron density using Eqs. (3, 1, 4), until convergence. The convergence criterion is determined and checked in terms of the evolution of the L_2 norm of the potential and density variations between subsequent iterations. Typically, the results are converged when the L_2 norms for the potential and density are on the order of 10^{-3} of the original values. Between subsequent iterations, we employ linear mixing in the electron density, according to

$$n'(x) = (1 - \alpha)n^{old}(x) + \alpha n^{new}(x), \quad (10)$$

where $n^{old}(x)$ is the input density to the Poisson solver, $n^{new}(x)$ is the new density obtained from the solution of the BTE using the new electric field obtained from the Poisson solver, and $n'(x)$ is the final density that is used as an input to the next iteration in the Poisson-Boltzmann loop. The convergence and stability of the self-consistent loop are strongly dependent on the system parameters and the nonequilibrium nature of the electronic system. If the system is strongly out of equilibrium, displaying large variations and strengths of the electric field, the mixing parameters α may have to be chosen as small as a few percent, thus affecting the overall runtime. Furthermore, for highly doped structures, the convergence is slower, partly due to the required small grid size in position due to the small Debye length, but also due to the slow convergence in the SOR procedure in the BTE, where the stability of the numerical scheme is given in terms of a Courant-Friedrich-Levy type condition [8]. Still, the computational demands for the calculations reported in this paper are modest.

4. Numerical results

In the following, we demonstrate our numerical approach with calculations of the transport characteristics of a model GaAs $n^+ - n^- - n^+ - n^- - n^+$ structure with the doping densities $n^+ = 10^{23} \text{ m}^{-3}$ and $n^- = 10^{19} \text{ m}^{-3}$. In order to highlight the effects of inhomogeneities and scattering while keeping the nature of the scattering structureless, we use a constant scattering time $\tau = 2.5 \cdot 10^{-13} \text{ s}$, which corresponds to realistic mobilities of GaAs at room temperature for which

the calculations have been performed. The central $n^- - n^+ - n^-$ region has the dimensions 200/200/200 nm, whereas the contacts are 1 μm long.

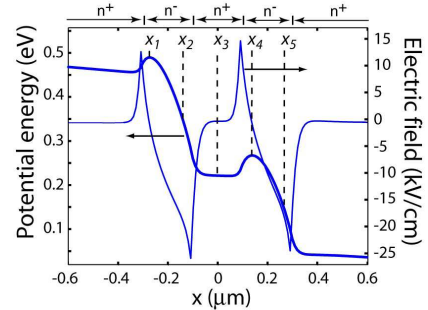


Figure 1: Electron potential energy and electric field in the central region of the $n^+ - n^- - n^+ - n^- - n^+$ system with dimensions described in the text. The corresponding current density is $j(x) = -5.4 \cdot 10^4 \text{ A/cm}^2$.

In Fig. 1 we show the electric field and potential energy around the central region of the system described above, subject to an applied bias voltage $V_b = -0.5 \text{ V}$. Due to the charge imbalance, electrons diffuse towards the lightly doped regions, where potential barriers are formed and, correspondingly, a large and inhomogeneous electric field on the order of 10 kV/cm is formed, even in the absence of an external applied voltage. As a finite voltage is applied to the device, the majority of the potential drop occurs over the submicron central region, giving rise to a strongly inhomogeneous field distribution, in contrast to the n^+ contact regions, where the field in comparison is very low and constant.

The electron velocity distribution in the central region of the structure is shown in Fig. 2(a), for five specific spatial points as depicted in Fig. 1. Figure 2(b) shows a contour plot of the full spatial dependence of $f(x, v)$ in that region. It is clear that the inhomogeneous electric field gives rise to a strong spatial dependence of the velocity distribution function along the direction of transport, and that the distribution function in the central region is very far from thermal equilibrium.

In the outermost highly doped n^+ regions, where the field is low and constant the distribution is simply a shifted Maxwellian. In the lightly doped n^- regions on the other hand, the velocity distribution is highly asymmetric and develops a narrow peak that rapidly shifts toward higher velocity along the direction of transport. This peak contains quasi-ballistic

electrons which are accelerated by the strong electric field in the central region, and thus, have a considerably larger average velocity compared to the electrons in the contacts. Close to the potential barrier the distribution function is suppressed at low velocities due to the skimming of the distribution of incoming electrons, as well as the restriction of drain induced electron flow with $v < 0$ due to the potential barrier.

However, the low-velocity contribution to the distribution function gradually increases away from the barrier, as thermionically injected electrons gradually are thermalized and the lower effective barrier height allows electrons from the n^+ regions to penetrate the lightly-doped region. Thus, the total distribution function consists of a quasi-ballistic, high-velocity and a diffusive, low-velocity contributions, which gives the total distribution function a highly non-Maxwellian broad and asymmetric shape. Furthermore, the presence of the two barriers creates an additional quasi-ballistic structure in the high-energy tail of the distribution function in the second n^- region, as electrons that traverse the intermediate n^+ region ballistically get an additional acceleration toward higher velocities by the electric field in the second n^- region, thus creating two high-velocity electron beams. These features emphasize the highly nonequilibrium nature of the electron transport in these type of systems and demonstrate that our method is capable of taking them fully into account.

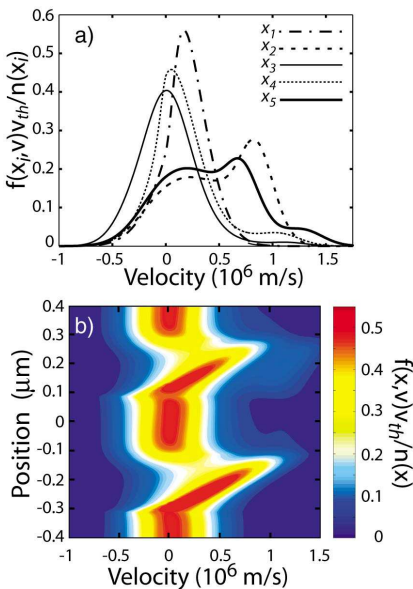


Figure 2: (Color online) Normalized electron velocity distribution function $f(x, v)v_{th}/n(x)$, where v_{th} is the thermal velocity, at (a) five different points in space corresponding to the points depicted in Fig. 1. (b) Contour plot of $f(x, v)v_{th}/n(x)$.

5. Conclusions

We have presented a numerical method for the solution of the steady-state, coupled Poisson-Boltzmann equations for the study of inhomogeneous, submicron semiconductor structures and demonstrated our approach on a submicron GaAs structure with strong built-in electric fields. We have shown that our method is capable of taking into account the strong nonequilibrium transport properties that arise in such systems due to the presence of very large and inhomogeneous electric fields, and that interesting structure is present in the high-energy tail of the distribution function, caused by quasi-ballistic electrons.

Acknowledgments

This work was supported by the Indiana 21st Century Research and Technology Fund.

References

Elements of this work have been summarized in an extended abstract published by IEEE.

1. C. Jacoboni, and P. Lugli, *The Monte Carlo Method for Semiconductor Device Simulation* (Springer-Verlag, Wien, 1989).
2. H. U. Baranger, and J. W. Wilkins, “Ballistic structure in the electron distribution function of small semiconducting structures: General features and specific trends,” *Physical Review B* **36**, 1487 (1987).
3. E. Fatemi, and F. Odeh, “Upwind finite difference solution of Boltzmann Equation applied to electron transport in semiconductor devices”, *Journal of Computational Physics* **108**, 209 (1993).
4. A. Majorana, and R. M. Pitadella, “A finite difference scheme solving the Boltzmann-Poisson system for semiconductor devices”, *Journal of Computational Physics* **174**, 649 (2001).
5. J.-H. Rhew *et al.*, “A numerical study of ballistic transport in nanoscale MOSFET”, *Solid State Electronics* **46**, 1899 (2002).
6. J. A. Carrillo *et al.*, “A WENO-solver for the transients of Boltzmann-Poisson system for semiconductor devices: performance and comparisons with Monte Carlo methods”, *Journal of Computational Physics* **184**, 498 (2003).
7. A. Majorana *et al.*, “Charge transport in 1D silicon devices via Monte Carlo simulation and Boltzmann-Poisson solver”, *COMPEL: The International Journal for Computation and Mathematics in Electrical and Electronic Engineering* **23**, 410 (2004).
8. W. H. Press *et al.*, *Numerical Recipes in C* (Cambridge University Press, Cambridge, 1992).